Smart Structures and Systems, *Vol. 16, No. 2 (2015) 243-262*
DOI: http://dx.doi.org/10.12989/sss.2015.16.2.243

Optimal sensor placement under uncertainties using a nondirective movement glowworm swarm optimization algorithm

Guang-Dong Zhou[1a], Ting-Hua Yi[*2,3], Huan Zhang[2b] and Hong-Nan Li[1c]

[1]*College of Civil and Transportation Engineering, Hohai University, Nanjing 210098, China*
[2]*School of Civil Engineering, Dalian University of Technology, Dalian 116024, China*
[3]*State Key Laboratory for Disaster Reduction in Civil Engineering, Tongji University, Shanghai 200092, China*

(Received February 12, 2014, Revised April 20, 2014, Accepted May 2, 2014)

Abstract. Optimal sensor placement (OSP) is a critical issue in construction and implementation of a sophisticated structural health monitoring (SHM) system. The uncertainties in the identified structural parameters based on the measured data may dramatically reduce the reliability of the condition evaluation results. In this paper, the information entropy, which provides an uncertainty metric for the identified structural parameters, is adopted as the performance measure for a sensor configuration, and the OSP problem is formulated as the multi-objective optimization problem of extracting the Pareto optimal sensor configurations that simultaneously minimize the appropriately defined information entropy indices. The nondirective movement glowworm swarm optimization (NMGSO) algorithm (based on the basic glowworm swarm optimization (GSO) algorithm) is proposed for identifying the effective Pareto optimal sensor configurations. The one-dimensional binary coding system is introduced to code the glowworms instead of the real vector coding method. The Hamming distance is employed to describe the divergence of different glowworms. The luciferin level of the glowworm is defined as a function of the rank value (RV) and the crowding distance (CD), which are deduced by non-dominated sorting. In addition, nondirective movement is developed to relocate the glowworms. A numerical simulation of a long-span suspension bridge is performed to demonstrate the effectiveness of the NMGSO algorithm. The results indicate that the NMGSO algorithm is capable of capturing the Pareto optimal sensor configurations with high accuracy and efficiency.

Keywords: structural health monitoring; optimal sensor placement; glowworm swarm optimization algorithm; information entropy; multi-objective optimization

1. Introduction

Large-scale civil infrastructures, i.e., long-span bridges, tall buildings or offshore platforms, are exposed to various environmental and service loads during their service life. Structural degradation and deterioration with time are an inevitable fact that may lead to structural failures and possible

*Corresponding author, Professor, E-mail: yth@dlut.edu.cn
[a] Assistant Professor, E-mail: zhougd@hhu.edu.cn
[b] Ph.D. Candidate, E-mail: hhuan1214@gmail.com
[b] Professor, E-mail: hnli@dlut.edu.cn

http://www.techno-press.org/?journal=sss&subpage=8 ISSN: 1738-1584 (Print), 1738-1991 (Online)

loss of human lives. To ensure structural safety and minimize financial loss, extensive evaluation is of pressing importance such that preventive and remedial work can be carried out as early as possible (Arangio and Beck 2012). Conventional visual inspection, which is experiential dependence, operation disturbance, and high costs, does not appear to be adequate to accurately reflect the true performance state of structural components or the global condition of the entire structure. In contrast, structural health monitoring (SHM) involves a paradigm of in situ data acquisition/sensing, data-feature extraction, and data-feature classification as a means of appropriately assessing the performance condition of a structure (Flynn and Todd 2010). Successful implementation and operation of SHM systems for large structures have been reported throughout the world (Yi *et al*. 2013, Zhou and Yi 2013a, Zhou and Yi 2013b).

In general, a typical SHM system includes three major components: a sensor system, a data processing system (including data acquisition, transmission and storage), and a health evaluation system (including diagnostic algorithms and information management) (Mufti 2002, Zhou and Yi 2013c). The performance of an SHM system relies heavily on the quantity and quality of the measured data, which in turn depend on the number of sensors used and their corresponding locations. It is well known that the number of sensors installed in a structure is always sparse compared with the infinite degrees of freedom (DOFs) of a structure. As a result, it is critical that researchers or engineers answer the question of where to place the sensors before performing any field tests (Chow *et al*. 2011). Therefore, the problem of optimal sensor placement (OSP) has received considerable attention in recent times. In extracting the OSP, an actual problem that should be solved is how to assess the performance of a sensor set. Many evaluation criteria were proposed from different perspectives, i.e., the modal assurance criterion (MAC), the singular value decomposition ratio (SVDR), and the measured energy per mode (Yi and Li 2012). The MAC suggested by Carne and Dohmann is a metric of linear independency such that the measured or identified modes are distinguishable (Carne and Dohmann 1995). The SVDR is adopted to evaluate the mode orthogonality, the condition for mode expansion, and the observability of the modes (Friswell and Mottershead 1995). The criterion of the measured energy per mode aids in selecting those sensor positions with possibly large amplitudes and in increasing the signal-to-noise ratio, which is critical in harsh and noisy circumstances. All of the aforementioned evaluation criteria assume that the measured data and the identified structural parameters are highly reliable and allocate little attention to the uncertainties in monitoring. However, it is worth noting that estimates of the structural parameters always involve uncertainties. Those uncertainties, which arise from various sources (i.e., the limitations of the mathematical models used to represent the behavior of the real structure, the incomplete measured data due to the limited sensor number, the presence of measurement error in the data, and insufficient excitation and response bandwidth (Beck and Katafygiotis 1998, Papadimitriou 2004, Li, *et al*. 2012a, Li, *et al*. 2012b)), may result in false alarms or genuine structural damage going undetected. In view of this situation, it is desirable to design the sensor configuration in an SHM system such that the structural parameters identified from the measured data are more robust to the uncertainties. Many research activities, i.e., the work by Ntotsios *et al.* (Ntotsios *et al.* 2005) and earlier works by Udwadia (Udwadia 1994) and Heredia-Zavoni *et al.* (Heredia-Zavoni *et al.* 1998), have shown the importance of addressing the issue of uncertainty in handling the optimal sensor configuration. In this paper, the information entropy (Papadimitriou *et al.* 2000, Yuen *et al*. 2001, Papadimitriou 2004, Chow *et al*. 2011, Ye and Ni 2012), which provides a direct measure of the uncertainties in the structural parameters, is used as the evaluation criterion of the OSP problem. Next, the information-entropy-based OSP problem is formulated as the multi-objective optimization problem of finding sensor sets that

minimize the information entropy indices because the responses of civil structures are always governed by several modes.

With respect to the traditional OSP problems with single-objective functions (evaluation criteria), many contributions have been developed in the past several decades and can be roughly divided into two categories. The first category contains the non-intelligent algorithms that use a closed-form process to find the best sensor set, i.e., the effective independence method (Kammer 1991) and MinMAC method (Carne and Dohmann 1995). The second category involves the intelligent algorithms that imitate the process of biological evolution, i.e., the genetic algorithm (GA) (Yao *et al.* 1993, Kang, *et al.* 2008, Yi *et al.* 2011a, Yi *et al.* 2011b, Zhou and Yi 2013d), or mimic the cooperative behavior of swarms, i.e., the ant colony optimization (ACO), the Artificial bee colony (ABC) (Kang, *et al.* 2013), the particle swarm optimization (PSO) (Ngatchou *et al.* 2005), and the monkey algorithm (MA) (Yi *et al.* 2012a, Yi *et al.* 2012b). These intelligent algorithms have been extensively applied to the OSP problem in recent years due to their many advantages over the classical optimization techniques, i.e., blind searching and highly parallel structure. All of the algorithms mentioned above focus on identifying a unique optimal sensor configuration. For the information-entropy-based OSP problem with multi-objective functions, it is impossible to find a solution that can optimize all of the objective functions because these objectives are conflicting. A compromise for the multi-objective problem involves investigating a set of solutions known as the Pareto solutions, each of which satisfies the objectives at an acceptable level without being dominated by any other solution. Papadimitriou proposed a Pareto sequential sensor placement (PA-SSP) algorithm for sequentially constructing predictions of the Pareto front and the Pareto optimal sensor configurations (Papadimitriou 2005). It was demonstrated that the PA-SSP could effectively find the Pareto optimal sensor configurations. However, when this method is applied in large-scale structures with hundreds of DOFs, e.g., long-span suspension bridges and spatial structures, its computational efficiency and accuracy are limited. The glowworm swarm optimization (GSO) algorithm, which is a recently developed meta-heuristic optimization method by Krishnanand and Ghose (Krishnanand and Ghose 2005), attracts great interest when it was presented and has many applications, i.e., numerical optimization calculation, the knapsack problem, wireless sensor networks deployment, multi-model function optimization, noise testing, simulation of the sensor machine crowd, and clustering analysis (Bharat 2008, Krishnanand and Ghose 2009, Yang *et al.* 2010, Gong *et al.* 2011, Liao *et al.* 2011, Zhou *et al.* 2013, Zainal *et al.* 2013). The GSO algorithm, which originated from simulating the natural functions of a glowworm swarm for foraging and seeking spouses, shares certain common features with the ACO algorithm and with the PSO algorithm but with several significant differences. Compared with the PSO algorithm, the ACO algorithm, and other traditional swarm intelligence optimization algorithms, the GSO algorithm offers many attractive properties, i.e., rapid computing speed, high efficiency, multi-point parallel global random searching without complex operations evolution, less adjustable parameters, and ease of realization (Huang *et al.* 2011, Nie *et al.* 2014). Up to now, this excellent algorithm has been only applied in single-objective optimization problems with continuous variables. This paper presents several improvements such that the concept of the GSO algorithm can be used for the information-entropy-based OSP problem.

This paper outlines a methodology for the OSP in SHM under uncertainty. The information-entropy-based OSP problem is first formulated with the purpose of finding the Pareto optimal sensor configurations that can minimize the uncertainties in estimated structural parameters. The information entropy that measures the uncertainty in the structural parameters is

introduced as the performance measure for the sensor configurations. The closed-form formulation of the objective functions that evaluates the uncertainties of the mode shapes before and after damage in the structure is specified. Next, a nondirective movement glowworm swarm optimization (NMGSO) algorithm deduced from the GSO algorithm is proposed for finding the Pareto optimal sensor configurations. The basic GSO algorithm (required in the description of the NMGSO algorithm) is reviewed. Selected improvements in the coding system, the Hamming distance, the luciferin definition, and the nondirective movement are detailed. A numerical simulation is performed to illustrate the effectiveness of the NMGSO algorithm, and the results are compared with those obtained from the PA-SSP algorithm.

2. Formulation of the optimal sensor placement problem

2.1 Damage detection method

The most important function of an SHM system implemented on a structure is condition assessment. Thus, the sensor configuration should use damage detection as a starting point. As usual, a continuous structure can be modeled using many discrete elements, and the damage in the structural elements can be assumed as a reduction of their entire stiffness matrix, whereas the other properties, i.e., mass, connectivity between elements, and damping ratio, remain unchanged. The reduction of the element stiffness matrix $\Delta\mathbf{K}_k$ can be expressed as (Shi *et al*. 2000, Ye and Ni 2012)

$$\Delta\mathbf{K}_k = \theta_k\mathbf{K}_k \quad (-1\leq\theta_k\leq 0) \tag{1}$$

where $\mathbf{K}_k$ and θ_k represent the stiffness matrix and the damage coefficient of the kth element, respectively. The damage coefficient θ_k is a value ranging from -1 and 0, and $\theta_k<0$ indicates that the element is damaged, whereas $\theta_k=0$ implies that the element is intact.

Because it is difficult to model the entire damage in a structure in sufficient detail for a general type of damage, the reduction of the global structure's stiffness matrix due to damage is assumed as the summation of the variations in each elemental stiffness matrix, i.e.,

$$\Delta\mathbf{K} = \sum_{k=1}^{L}\Delta\mathbf{K}_k = \sum_{k=1}^{L}\theta_k\mathbf{K}_k \tag{2}$$

where L denotes the total number of elements in the model. This model is suitable for most types of damage in actual structures and works even for damage in which change is not proportional to the elemental stiffness because this assumption gives only a small error for a large structure and does not change the essence of the requirements for damage localization. Next, the change of the ith mode shape due to the damage can be represented as the summation of the contribution of each local damage in the structure (Shi *et al*. 2000)

$$\Delta\boldsymbol{\phi}_i(\boldsymbol{\theta}) = \sum_{k=1}^{L}\theta_k\sum_{\substack{r=1\\ r\neq i}}^{N}\frac{-\boldsymbol{\phi}_r^T\mathbf{K}_k\boldsymbol{\phi}_i}{\omega_r^2-\omega_i^2}\boldsymbol{\phi}_r \triangleq \mathbf{F}_i(\mathbf{K})\boldsymbol{\theta} \tag{3a}$$

$$\boldsymbol{\theta} = \{\theta_1 \quad \theta_2 \quad \cdots \quad \theta_L\}^T \tag{3b}$$

$$\mathbf{F}_i(\mathbf{K}) = [\mathbf{F}_i(\mathbf{K}_1)\ \mathbf{F}_i(\mathbf{K}_2)\ \cdots\ \mathbf{F}_i(\mathbf{K}_k)\ \cdots\ \mathbf{F}_i(\mathbf{K}_L)] \tag{3c}$$

$$\mathbf{F}_i(\mathbf{K}_k) = \sum_{\substack{r=1 \\ r\neq i}}^{N} \frac{-\phi_r^T \mathbf{K}_k \phi_i}{\omega_r^2 - \omega_i^2}\phi_r \tag{3d}$$

where $\Delta\phi_i$ denotes the measured mode shape change matrix, N is the number of DOFs of the model, ω_i and ϕ_i represent the ith mode frequency and mode shape of the undamaged structure, respectively, $\mathbf{F}_i(\mathbf{K})$ is defined as the sensitivity matrix for the ith mode shape, and $\boldsymbol{\theta}$ denotes the damage coefficient vector.

2.2 Information-entropy-based optimal sensor placement

Theoretically, the optimal estimate of the damage coefficient vector $\hat{\boldsymbol{\theta}}$ can be obtained from Eq. (3) once the mode shapes before and after damage to the structure are identified via the measured data. Additionally, the damage of the structure can be detected. However, it is well known that the measured mode shapes are contaminated by various sources (i.e., incomplete measured data due to limited sensor number, measurement noise, modeling error, and insufficient bandwidth of excitation and response), which induce uncertainties in the estimated structural parameters and subsequently result in false identification of the structural condition. Many research studies have shown the significance of uncertainties in SHM (Azarbayejani *et al*. 2008). In particular, these uncertainties are connected with the data obtained from a sensor set that is located in the structure. Because the information entropy provides a unique scalar measure of the uncertainty in the estimate of the structural parameters, the optimal sensor configuration should be the one that minimizes the information entropy. Therefore, the problem of finding the optimal sensor placement is formulated as a discrete optimization problem with the objective function of minimal information entropy.

Based on the Bayesian statistical system identification methodology developed by Beck and Katafygiotis (Beck and Katafygiotis 1998), the measured change of the ith mode shape of the structure is

$$\Delta\varphi_i(m;\boldsymbol{\theta}) = \mathbf{L}_0(\boldsymbol{\delta})\Delta\phi_i(m;\boldsymbol{\theta}) + \mathbf{L}_0(\boldsymbol{\delta})\mathbf{n}(m;\boldsymbol{\theta}) \tag{4}$$

where m=1, …, N is the sample series of the measured time history, $\Delta\varphi_i(m;\boldsymbol{\theta}) \in \mathbf{R}^{N_0}$ is the ith measured mode shape change for the damage coefficient vector $\boldsymbol{\theta}$, $\Delta\phi_i(m;\boldsymbol{\theta}) \in \mathbf{R}^{N_d}$ represents the ith predicted mode shape change in Eq. (3), N_0 and N_d are the number of measured DOFs and the number of measurable DOFs, respectively, $\mathbf{L}_0(\delta) \in \mathbf{R}^{N_0 \times N_d}$ denotes the observation matrix composed of zeros and ones and maps the measured DOFs to the measurable DOFs, $\boldsymbol{\delta} \in \mathbf{R}^{N_d}$ is the sensor configuration vector specifying the N_0 measured DOFs with δ_j=1 at the observed DOF and δ_j=0 at the unobserved DOF, and $\mathbf{n} \in \mathbf{R}^{N_d}$ denotes the prediction error concerning the damage coefficient vector $\boldsymbol{\theta}$. The observation matrix satisfies the relationship $\mathbf{L}_0^T\mathbf{L}_0 = diag(\delta)$.

The uncertainties of the estimated damage coefficient vector $\boldsymbol{\theta}$ are measured by the information entropy $H(D)$, which is defined as (Jaynes 1978)

$$H(D) = \mathrm{E}_{\theta}[-\ln\ p(\boldsymbol{\theta} \mid D)] = -\int p(\boldsymbol{\theta} \mid D) \ln\ p(\boldsymbol{\theta} \mid D) d\boldsymbol{\theta} \tag{5}$$

where D is the measured data, E_{θ} denotes the mathematical expectation with respect to $\boldsymbol{\theta}$, and $p(\boldsymbol{\theta}|D)$ represents the probability density function specifying the plausibility of each possible value of the damage coefficient vector $\boldsymbol{\theta}$, which provides a spread of the uncertainty in the damage coefficient vector based on the information contained in the measured data.

According to the asymptotic approximation, which is valid for large number of data ($N \to \infty$) as proved by Papadimitriou (Papadimitriou 2004), the information entropy only depends on the sensor configuration vector $\boldsymbol{\delta}$, the optimal damage coefficient vector $\hat{\boldsymbol{\theta}}$, and the optimal prediction error $\hat{\sigma}$, and it is independent of the time-history details of the measured data D. However, in practice, since the data are not available in the initial stage of designing the monitoring system, an estimate of the optimal model parameters $\hat{\boldsymbol{\theta}}$ and $\hat{\sigma}$ cannot be obtained. Thus, to proceed with the design of the optimal sensor configuration, it is assumed that the optimal model parameters $\hat{\boldsymbol{\theta}}$ and $\hat{\sigma}$ are replaced by certain nominal values $\boldsymbol{\theta}_0$ and σ_0 chosen by the designer as representative of the structure. In this way, the information entropy in Eq. (5) takes the form

$$H(D) \sim H(\boldsymbol{\delta}, \boldsymbol{\theta}_0, \sigma_0) = \frac{1}{2} N_{\boldsymbol{\theta}} [\ln(2\pi) + \ln \sigma_0^2] - \frac{1}{2} \ln(\det\ \mathbf{Q}(\boldsymbol{\delta}, \boldsymbol{\theta}_0)) \tag{6}$$

where N_{θ} represents the number of damage coefficients for the measured data. The matrix $\mathrm{Q}(\boldsymbol{\delta}, \boldsymbol{\theta}_0)$ is a positive semi-definite matrix, known as the Fisher information matrix, and is given by

$$\mathbf{Q}(\boldsymbol{\delta}, \boldsymbol{\theta}_0) = \sum_{j=1}^{N_d} \delta_j \mathbf{P}^{(j)}(\boldsymbol{\theta}_0) \tag{7}$$

The matrix $\mathrm{Q}(\boldsymbol{\delta}, \boldsymbol{\theta}_0)$ contains the information on the values of the parameters $\boldsymbol{\theta}$ based on the data from all measured positions specified in $\boldsymbol{\delta}$. The matrix $\mathbf{P}^{(j)}(\boldsymbol{\theta}_0)$ is a positive semi-definite matrix of the form (Ye and Ni 2012)

$$\mathbf{P}^{(j)}(\boldsymbol{\theta}_0) = \nabla_{\boldsymbol{\theta}} [\Delta\phi_{ij}(\boldsymbol{\theta}_0)] \nabla_{\boldsymbol{\theta}}^T [\Delta\phi_{ij}(\boldsymbol{\theta}_0)] \tag{8}$$

where $\Delta\phi_{ij}$ is the jth element of the ith mode shape change of the structure, and $\nabla_{\boldsymbol{\theta}} = [\partial/\partial\theta_1 \quad \cdots \quad \partial/\partial\theta_{N_{\boldsymbol{\theta}}}]^T$ is the usual gradient vector with respect to the parameter vector $\boldsymbol{\theta}$. The matrix $\mathbf{P}^{(j)}(\boldsymbol{\theta}_0)$ represents the contribution of each DOF measurement to the change of modal behavior due to the damage. Substituting $\Delta\phi_{ij}$ given in Eq. (3) into Eq. (8), the $\mathbf{P}^{(j)}(\boldsymbol{\theta}_0)$ can be derived as follows

$$\mathbf{P}^{(j)}(\boldsymbol{\theta}_0) = \mathbf{F}_i^{(j)}(\mathbf{K}) \mathbf{F}_i^{(j)T}(\mathbf{K}) \tag{9}$$

where $\mathbf{F}_i^{(j)}(\mathbf{K})$ denotes the jth row in the matrix $\mathbf{F}_i(\mathbf{K})$.

It can be found from Eq. (9) that the damage coefficient vector $\boldsymbol{\theta}$ is eliminated through the gradient vector ∇_{θ}, and the matrix $\mathbf{P}^{(j)}(\boldsymbol{\theta}_0)$ is independent of the nominal values $\boldsymbol{\theta}_0$. Therefore, the Fisher information matrix can be estimated from the structural stiffness matrix and mode

shapes without damage involving the different sensor configurations. Subsequently, the information entropy is only associated with the sensor configuration $\boldsymbol{\delta}$ and the designed prediction error σ_0, and thus, it can directly measure the uncertainties in the structural parameters for different sensor configurations. In other words, the information entropy provides a rational criterion with which to evaluate the uncertainties of different sensor configurations in the structural condition assessment. For simplicity, the information entropy index $IEI_i(\boldsymbol{\delta})$ for the ith measured mode shape is introduced as a measure of the effectiveness of a sensor configuration $\boldsymbol{\delta}$, which is defined as follows (Papadimitriou 2005)

$$IEI_i(\boldsymbol{\delta}) = \frac{H_i(\boldsymbol{\delta}) - H_i(\boldsymbol{\delta}_{\text{ref}})}{H_i(\boldsymbol{\delta}_{0,\text{ref}}) - H_i(\boldsymbol{\delta}_{\text{ref}})} \tag{10}$$

where $H_i(\boldsymbol{\delta}_{\text{ref}})$ and $H_i(\boldsymbol{\delta}_{0,\ \text{ref}})$ are the information entropies computed for two referenced sensor configurations $\boldsymbol{\delta}_{\text{ref}}$ and $\boldsymbol{\delta}_{0,\ \text{ref}}$, respectively. The $H_i(\boldsymbol{\delta}_{\text{ref}})$ is calculated from the best sensor configuration that results in the minimum information entropy, whereas the $H_i(\boldsymbol{\delta}_{0,\ \text{ref}})$ is computed from the worst sensor configuration that yields the maximum information entropy. In this case, the values of $IEI_i(\boldsymbol{\delta})$ range from zero to one. The most effective configuration corresponds to a value of $IEI_i(\boldsymbol{\delta})$ equal to zero, and the least effective configuration corresponds to a value of $IEI_i(\boldsymbol{\delta})$ equal to one.

Due to the complexity of civil structures, only one mode shape is insufficient for structural condition evaluation. If we let $J_i = IEI_i(\boldsymbol{\delta})$, the information entropy index including u objectives will produce

$$\mathbf{J}(\boldsymbol{\delta}) = (J_1(\boldsymbol{\delta}), J_2(\boldsymbol{\delta}), \cdots, J_u(\boldsymbol{\delta})) \tag{11}$$

The optimal sensor configuration is the one that has the minimal $\mathbf{J}(\boldsymbol{\delta})$. As a result, the OSP problem becomes a multi-objective optimization problem. Instead of a single objective, there is a set of conflicting objective for which no unique optimal solution satisfies all objectives. Alternatively, a set of solutions exists that is optimal in the sense that no other solutions in the search space are superior if all objectives are considered. The alternative solutions that trade off the information entropy values for different mode shapes are known as the Pareto optimal solutions in multi-objective optimization problems and are also referred to as the Pareto optimal sensor configurations in OSP problems.

It is necessary to introduce certain useful terminologies that appear in the multi-objective optimization problem (Fonseca and Fleming1995, Konak *et al*. 2006). Specifically, a feasible solution $\mathbf{a} \in \boldsymbol{\delta}$ is said to dominate a feasible solution $\mathbf{b} \in \boldsymbol{\delta}$ (also written as $\mathbf{a} \prec \mathbf{b}$) if and only if

$$J_i(\mathbf{a}) \le J_i(\mathbf{b}) \qquad \forall i \in \{1, \cdots u\} \ \text{ and } \ \exists j \in \{1, \cdots, u\} : J_j(\mathbf{a}) < J_j(\mathbf{b}) \tag{12}$$

A solution is said to be a Pareto optimal solution if it is not dominated by any other solution in the solution space. A Pareto optimal solution cannot be improved with respect to any objective without worsening at least one other objective. The set of all feasible non-dominated solutions in $\boldsymbol{\delta}$ is referred to as the Pareto optimal set, and for a given Pareto optimal set, the corresponding objective function values in the objective space are known as the Pareto front.

To find the Pareto optimal sensor configurations, a method known as the PA-SSP algorithm was developed by Papadimitriou (Papadimitriou 2005). The PA-SSP algorithm places the N_0 sensors one by one. The feasible solutions for one sensor are first determined by placing one

sensor on each measurable DOF. Those dominated configurations are deleted by Eq. (12), and the Pareto optimal sensor configurations are extracted. The Pareto optimal sensor configurations for (v+1) sensors are thus obtained iteratively from the Pareto optimal sensor configurations for v sensors as follows. Let $P_v^{n_v}$ be the set of all Pareto solutions for v sensors, where n_v is the solution number. For each solution, a new set of all possible sensor configurations involving (v+1) sensors is constructed by adding one more sensor at each unobserved measurable DOF. Next, the Pareto solutions for (v+1) sensors are obtained by deleting those solutions **b** that satisfy Eq. (12). This iteration process is continued for up to N_0 sensors. It can be observed that the PA-SSP algorithm will accurately predict the Pareto optimal sensor configurations only in the case for which the sensor locations of any Pareto optimal sensor configuration involving v sensors is a subset of the locations of at least one of the Pareto optimal sensor configurations involving (v+1) sensors. However, the last argument does not apply in general, and the sensor configurations computed by the PA-SSP algorithm cannot be guaranteed to be the exact Pareto optimal solutions. At the vth iteration, the number of generated feasible sensor configurations is $(N_d-v)n_v$. Let N_d, v, and n_v be equal to 500, 10, and 40, respectively, values that are entirely possible in large structures. The $(N_d-v)n_v$ is thus equal to 19, 600. Extracting the Pareto optimal solutions from so many feasible configurations is undoubtedly a challenging task, and furthermore, the work is repeated N_0 times. The greater the number of mode shapes involved in the algorithm, the more complex the computation will be. Therefore, the PA-SSP algorithm has low efficiency for large-scale structures. To improve the computational efficiency, many of the Pareto solutions must be pruned by means of clustering, and as a result, many meaningful sensor configurations are lost. Therefore, it is necessary to propose a methodology for this OSP problem that offers higher accuracy and higher efficiency.

3. Nondirective movement glowworm swarm optimization algorithm

3.1 Basic glowworm swarm optimization algorithm

The inspiration for the basic GSO algorithm originates from the phenomenon by which one glowworm is attracted by another that has a higher quantity of a luminescent known as luciferin and consequently moves toward it. In nature, glowworms communicate with each other by releasing luciferin. Glowworms attract others around them by giving off fluorescent light. The higher the concentration of luciferin, the greater the intensity of fluorescence, and the glowworm is thus able to attract additional glowworms. The GSO algorithm simulates this phenomenon (Zhou *et al*. 2013).

In the GSO algorithm, the glowworms are initially randomly distributed in the search space, which contains an equal and constant luciferin value, l_0. The glowworm emits light with an intensity is proportional to the amount of associated luciferin and interacts with other glowworms within a variable neighborhood. In particular, the neighborhood is defined as a local-decision domain that has a variable neighborhood range r_d^s bounded by an ultimate range r_u ($0 \le r_d^s \le r_u$). A glowworm s assigns another glowworm k as its neighbor only if k is within the neighborhood range of s and the luciferin level of k is higher than that of s. Each glowworm is attracted by the brighter glow of other glowworms in the neighborhood and subsequently selects a neighbor using a probabilistic mechanism to move toward it. Generally, the basic GSO algorithm includes three

stages: luciferin update phase, movement phase, and neighborhood range update phase (Krishnanand and Ghose 2009).

3.1.1 Luciferin updating

During the luciferin update phase, each glowworm changes its luciferin value according to the objective function value of its current location. The luciferin update rule is given by

$$l_s(t+1) = (1-\rho) l_s(t) + \gamma J\left(C_s(t+1)\right) \tag{13}$$

where $l_s(t)$ represents the luciferin level associated with glowworm s at time t, ρ ($0<\rho<1$) is the luciferin decay constant, γ denotes the luciferin enhancement constant, and $J(C_s(t))$ indicates the objective function value of the glowworm s at time t.

3.1.2 Movement

Using a probabilistic mechanism, each glowworm decides to move toward a neighbor that has a luciferin value higher than its own, i.e., glowworms are attracted by neighbors with brighter glow. For each glowworm s, the probability of moving toward a neighbor k is

$$p_{sk}(t) = \frac{l_k(t) - l_s(t)}{\sum_{e \in N_s(t)} \left[l_e(t) - l_s(t) \right]} \tag{14}$$

where $e \in N_s(t)$, $N_s(t)=\{e:\ d_{se}(t) \le r_d^s(t)\ ,\ l_s(t)<l_e(t)\}$ is the set of neighbors of glowworm s at time t, $d_{se}(t)$ represents the Euclidean distance between glowworms s and e at time t, and $r_d^s(t)$ denotes the variable neighborhood range associated with glowworm s at time t. After the glowworm s selects a glowworm $k \in N_i(t)$ as a target, the glowworm movements can be stated as

$$C_s(t+1) = C_s(t) + st\left(\frac{C_k(t) - C_s(t)}{\left\| C_k(t) - C_s(t) \right\|} \right) \tag{15}$$

where $C_s(t) \in \mathbf{R}^m$ is the location of glowworm s at time t in the m-dimensional real space $\mathbf{R}^m$, $\left\| \cdot \right\|$ represents the Euclidean norm operator, and st (>0) is the step size.

3.1.3 Neighborhood range updating

As the position of the glowworm changes, its neighborhood range is correspondingly updated to restrict the neighbor number of glowworm s and improve the computational efficiency. If the neighborhood range covers a low density of glowworms, the neighborhood range is extended. In the opposite situation, the neighborhood range is reduced. The formula for the neighborhood range update is expressed as follows

$$r_d^s(t+1) = \min\{\, r_u, \max\{0, r_d^s(t) + \beta(n_g - \left| n_{N_s(t)} \right|)\}\} \tag{16}$$

where β represents a constant parameter, n_g is a parameter used to control the neighbor number, and $n_{N_s(t)}$ is the neighbor number of glowworm s at time t.

Code→	0	0	1	1	0	0	1	0
DOF→	1	2	3	4	5	6	7	8

Fig. 1 Permutation of a code

3.2 Nondirective movement glowworm swarm optimization algorithm

The basic GSO algorithm was originally designed to solve global numerical optimization problems with continuous variables and uses the real vectors to represent the locations of glowworms. However, for the problem at hand, the optimization variables are constrained by whether the DOFs are occupied by sensors, which cannot be expressed using spatial coordinates. Thus, the real coding system is unsuitable for the OSP problem. Accordingly, the Euclidean distance and the movement strategy defined in the basic GSO algorithm are no longer unavailable. In this section, selected improvements involving the coding system, distance between glowworms, luciferin definition, and movement scheme are developed such that the heuristic conception of the GSO algorithm can be applied in the OSP problems.

3.2.1 Coding system

From the viewpoint of mathematics, the model of the OSP is a 0-1 programming problem. Thus, the design variables in the OSP can be coded using a simple one-dimensional binary coding system. This coding system is quite simple and intuitive and is extensively used in the GAs. In this coding system, each glowworm represents a solution (i.e., a feasible sensor configuration) and is analogous to the chromosome that represents an individual in the GA. The location of glowworm s is modeled as a permutation $C_s=\{c_{s,1}, c_{s,2}, \ldots, c_{s,\eta}, \ldots, c_{s,N_d}\}$, where N_d is the number of measurable DOFs. In the permutation, the values of the elements represent the condition of the sensor placement, the sequence represents the serial number of DOFs, $c_{s,\eta}=1$ means that a sensor is located on the ηth DOF, and $c_{s,\eta}=0$ indicates that no sensor is placed on the ηth DOF. For example, one code is shown in Fig. 1. This code indicates that there are eight measurable DOFs, among which the 3rd, 4th, and 7th are occupied by sensors. When initializing a glowworm, its binary permutation is firstly produced randomly and further reorganized by the shuffle method.

3.2.2 Distance between glowworms

The Euclidean distance is no longer meaningful if it is applied in the one-dimensional binary coding system. The Hamming distance, which is used in telecommunications to count the number of flipped bits in a fixed-length binary word as an estimation of error, is a good tool for describing the distance between glowworms that are coded by the one-dimensional binary coding system. The Hamming distance is named for Richard Hamming, who introduced it in his fundamental paper on Hamming codes, "Error detecting and error correcting codes", in 1950 (Hamming 1950); this measure is also known as the signal distance. The Hamming distance between two permutations of equal length is the number of positions at which the corresponding symbols are different. For glowworms s and k with binary strings, the Hamming distance can be expressed as

$$d_{sk} = C_s \oplus C_k = (C_s \vee C_k) \wedge \neg(C_s \wedge C_k) \tag{17}$$

where C_s and C_k denote the codes of glowworm s and glowworm k, respectively, $\oplus$ is XOR, $\vee$ is the logical disjunction, $\wedge$ represents a logical conjunction, and $\neg$ denotes logical negation.

The underlying concept of the Hamming distance is that it represents the incongruous sensors and is equal to the number of ones in glowworm s XOR glowworm k and zeros in glowworm s XOR glowworm k. Thus, the Hamming distance between glowworms s and k can be rewritten as

$$d_{sk} = C_s \oplus C_k = \sum_{\eta=1}^{N_d} \left| c_{s,\eta} - c_{k,\eta} \right| \tag{18}$$

It should be noted that the distance d_{sk} defined by Eq. (18) is always a nonnegative even number, which is beneficial for establishing the movement scheme for the reason that the total number of ones (which is equal to the predetermined sensor number) in any binary string of glowworms is the same. The number of ones in glowworm s that have sensor locations that differ from glowworm k is equal to the number of sensors in glowworm s that are located in different DOFs from glowworm k. The maximum value of d_{sk} is $2N_0$, which means that the sensors of glowworm s and the solution of glowworm k occupy different DOFs in a structure. If the minimum value of d_{sk} is zero, this that means that the solution of glowworm s is the same as that of glowworm k. As a result, the interval of distance d_{sk} is $[0, 2N_0]$. Taking the two solutions for glowworms s and k shown in Fig. 2 as an example, the number of ones in glowworm s that are different from glowworm k is two, which is equal to the number of zeros in glowworm s that are different from glowworm k. The number of incongruous sensors is four, and therefore, the distance between glowworm s and glowworm k is four.

3.2.3 Luciferin definition

The neighbors of glowworm s in the basic GSO algorithm are defined as those glowworms that have higher luciferin levels within the neighborhood range. The luciferin level calculated by Eq. (13) is associated with the objective function. In multi-objective optimization problems, the objective function includes several values that conflict with each other. As a result, the luciferin level becomes a vector, which cannot be directly compared. In this work, the non-dominated sorting strategy (Deb *et al*. 2002) is adopted.

Once the glowworms are located, the glowworms are sorted based on non-domination into each front, i.e., the Pareto front. The first front is a completely non-dominant set in the current population, also referred to as the Pareto front, and the second front is only dominated by the glowworms in the first front. With repetition, all fronts are formed. Each glowworm is assigned a rank value (RV) based on the front to which it belongs. For examples, the glowworms in the first front are given a RV of 1, the glowworms in second front are assigned an RV of 2, etc.

Glowworm $s\rightarrow$	1	0	1	0	1	1	0	1
Glowworm $k\rightarrow$	1	1	1	1	1	0	0	0

Fig. 2 Two solutions for glowworm s and glowworm k

To compare the glowworms that belong to the same front, a new parameter known as the crowding distance (CD) is employed. The CD is a measure of how close a glowworm is to its neighbors. A large average crowding distance will result in better diversity in the population. Each glowworm in the population is assigned a CD value. The CD is only effective within the same front. Comparison of the CD between two glowworms in different fronts is meaningless. The CD computation requires sorting the glowworms within the same front according to each objective function value in ascending order of magnitude. Thereafter, for each objective function, the boundary glowworms (glowworms with the smallest and largest function values) are assigned an infinite distance value. All other intermediate glowworms are assigned a distance value equal to the absolute normalized difference in the function values of two adjacent glowworms. This calculation is continued with the other objective functions. The overall CD value is calculated as the sum of the individual distance values corresponding to each objective. Each objective function is normalized within the same front before calculating the CD (Deb *et al*. 2002). The normalized objective function is calculated as

$$\left\langle J_i(s)\right\rangle = \frac{J_i(s)}{J_i^{\max} - J_i^{\min}} \tag{19}$$

where $\left\langle J_i(s)\right\rangle$ is the *i*th normalized objective function of glowworm *s*, and $J_i^{\max}$ and $J_i^{\min}$ represent the maximum value and the minimum value of the *i*th objective function, respectively.

Next, the luciferin level can be defined as a function of the RV and CD, which is

$$l_s(t) = -RV_s(t) + \frac{CD_s(t)}{CD_{RV_s}^{\max}(t)} \tag{20}$$

where $RV_s(t)$ represents the RV of glowworm *s* at time *t*, $CD_s(t)$ denotes the CD of glowworm *s* at time *t*, and $CD_{RV_s}^{\max}(t)$ is the maximum CD in the RVth front. If there are infinite distance values in the front, the infinite distance values are reset to $(1+\varepsilon)CD_{RV}^{\max}(t)$, where $CD_{RV}^{\max}(t)$ is the maximum CD in the RVth front except for the infinite distance values, and ε is a small nonnegative number (i.e., 0.03). In this manner, the infinite distance values can be differentiated from the $CD_{RV_s}^{\max}(t)$ and the Eq. (20) can be applied harmoniously. Under this definition, the luciferin levels of the glowworms that belong to the first front lie in the interval [-1, 0], the luciferin levels of the glowworms that belong to the second front lie in the interval [-2, -1], etc, and thus, the glowworms that belong to different RVs can be distinguished, and the glowworms that belong to the same RV are comparable. At the beginning of each iteration, the luciferin levels of the glowworms are re-calculated using Eq. (20) according to their current RVs and CDs.

After the movements of all glowworms are finished, all glowworms at time *t*-1 and time *t* are combined into a larger population. Non-dominated sorting is implemented again, and the glowworms in the larger population are sequenced according to their luciferin levels. The front half of the larger population is selected as the population at time *t*+1. As a result, the elitist glowworms are preserved.

3.2.4 Nondirective movement

Since the locations of the glowworms in the basic GSO algorithm are continuous variables, the

movement defined by Eq. (15) can be easily implemented. However, in the OSP problems, the locations of the glowworms are coded with the one-dimensional binary coding system, and a solution represents a feasible sensor configuration. Therefore, the movement of a glowworm is only realized by changing the value of the elements in the binary permutation, which implies relocating the sensors. In this manner, the number of elements that changed from zero to one or from one to zero can be viewed as the movement distance. Obviously, the movement distance is a nonnegative integer. Another important issue is that the total number of sensors that must be placed is predetermined and cannot be changed in the process of movement. For a specific binary permutation, the number of elements changed from zero to one must be equal to the number of elements changed from one to zero. This work proposes a nondirective movement scheme that relocates certain incongruous sensors.

Assume that glowworm k selected by Eq. (14) is the target of glowworm s, and the distance between glowworm s and glowworm k is d_{sk}. Therefore, the step size st_{sk} is

$$st_{sk} = random(1, d_{sk}/2)d_{sk} \tag{21}$$

where $random(\cdot)$ means random selection of an integer in the interval [1, d_{sk} /2]. Next, the following is obtained by substituting Eq. (21) into Eq. (15)

$$C_s(t+1) = C_s(t) + \tau_{sk}\left(C_k(t) - C_s(t)\right) \tag{22}$$

where $\tau_{sk}=random(1, d_{sk}/2)$ denotes the movement distance. Generally, the contribution of a sensor located on a DOF to the objective function cannot be pre-determined, and therefore, it is difficult to choose the relocated sensors such that the objective function is ameliorated. In the current paper, an alternate method is employed as follows:

(1) Calculate the difference between the permutations of glowworm s and glowworm k

$$\Delta C_{ks} = C_k - C_s \tag{23}$$

(2) Randomly select τ_{sk} elements whose value is 1 from ΔC_{ks} and change those elements to -1; again, randomly select τ_{sk} elements whose value is -1 from ΔC_{ks} and change those elements to 1. The operated ΔC_{ks} is represented by $[\Delta C_{ks}]$.

(3) Substitute $[\Delta C_{ks}]$ into Eq. (22), and the relocated glowworm s becomes

$$C_s(t+1) = C_s(t) + [\Delta C_{ks}] \tag{24}$$

Because the relocated sensors are selected randomly, the movement is nondirective. Superficially, this movement scheme may deviate from the concept of the basic GSO algorithm, but it should be pointed out that those movements are able to retain the glowworm diversity that is of extraordinary importance for multi-objective optimization problems.

A flow chart explaining the NMGSO algorithm used to find the Pareto optimal sensor configurations is shown in Fig. 3.

4. Numerical simulation

4.1 Bridge description

NONDIRECTIVE MOVEMENT GLOWWORM SWARM OPTIMIZATION ALGORITHM

Load structural parameters
Compute information entropy **J** by Eq. (11)
Set parameters r_u, r_0, β, and n_g
Set number of glowworms = N_g
Initialize glowworms
Let $C_s(t)$ be the location of glowworm s at time t
for s = 1 to N_g do: % Non-dominated sorting
{
$r_d^s(0) = r_0$
Assign RV
Calculate CD
}
Compute luciferin level
Set maximum iteration number = *iter_max*;
Set t = 1;
while *($t \le$ iter_max)* do:
{
  for each glowworm i do: % Movement
  {
    $N_s(t) = \{k : \ d_{sk}(t) \le r_d^s(t)$; and $l_s(t) < l_k(t)\}$;
    For each glowworm $k \in N_s(t)$

$$p_{sk}(t) = \frac{l_k(t) - l_s(t)}{\sum_{e \in N_s(t)} \left[l_e(t) - l_s(t) \right]}$$

    k = selected glowworm ($\vec{p}$)

$$C_s(t+1) = C_s(t) + \tau_{sk}\left(C_k(t) - C_s(t)\right)$$

$$r_d^s(t+1) = \min\{ r_s, \max\{ 0, r_d^s(t) + \beta(n_g - \left| n_{N_s(t)} \right|)\}\}$$

  }
  Computer information entropy **J** of all moved glowworms
  Combine all glowworms at time t-1 and all glowworms at time t
  for s = 1 to $2N_g$ do: % Non-dominated sorting
  {
  Assign RV
  Calculate CD
  }
  Compute luciferin level
  Select the top N_g glowworms as the next generation
  $t \leftarrow t + 1$;
}

Fig. 3 Flowchart of the process of establishing the Pareto optimal sensor configurations

To demonstrate the effectiveness of the proposed NMGSO algorithm, a long-span suspension bridge that crosses the Yangtze River in China is used as a numerical example. The main span of the bridge is 1,490 m and the two side spans are each 470 m in length. A full-joint streamlined flat

steel box girder is employed as the main girder. The steel box girder is 36.3 m wide and 3.0 m high, and its upper deck and bottom deck are 14 mm and 10 mm thick, respectively. The main cable is composed of 184 prefabricated parallel subsection cables, and each subsection cable contains 127 high-strength steel wires.

A total of 182 suspenders are used to transfer the loads from the box girder to the main cables. Each of the two gate-shaped towers consists of two rectangular single-box single-chamber reinforced concrete columns and three pre-stressed concrete crossbeams. The heights of the two towers are approximately 210 m (Zhou and Yi 2013c). A three-dimensional finite element model is established to provide input data for the OSP. The main girder and main towers are simulated by spatial beam elements, and the main cables and suspenders are simulated by 3D linear elastic truss elements with three DOFs at each node. The main girder is modeled with 92 elements and 93 nodes. The length of each element of the main girder is approximately 16.1 m. The model is updated based on field measurement data. The mode shapes that are necessary for calculation of the information entropy are obtained using modal analysis. These results are not shown for brevity and can be found in (Zhou and Yi 2013c). The first vertical modal frequency is only 0.08979 Hz, which reveals the notably low stiffness of this long-span suspension bridge. Therefore, conducting SHM and condition assessment is significant.

4.2 Results and discussion

Although many simplifications are applied, the finite element model of the bridge has a large number of DOFs. Only the vertical DOFs of the main girder are considered for possible sensor placement in this case study because the vertical vibration of the main girder is the representative dynamic response of the entire bridge. Consequently, a total of 93 DOFs are available for sensor placement (i.e., N_d=93). The values of parameters r_u, r_0, β, n_g, and N_g are problem specific. After extensive numerical experiments, it is suggested that the parameter r_u and r_0 can be selected as three-quarters and one-half of the N_0, respectively. According to the characteristics of the information-entropy-based OSP problem involving multi-objective functions, the parameters β and n_g are defined as approximately 0.03 and 100, respectively. The number of glowworms N_g is set to 200 in this simulation, which was found to be sufficient for achieving the best performance. Because maintaining the diversity of the population is important to multi-objective optimization problems, increasing the number of glowworms is beneficial to finding the Pareto front with less iterations.

The optimal sensor configurations are also computed using the PA-SSP algorithm to facilitate comparisons in terms of computational accuracy and efficiency. To display the outcomes intuitively, only the first two objective functions are taken into account. The partial Pareto points for 1, 3, 5, 10, 20, and 30 sensors are shown in Figs. 4(a)-4(f), respectively. These figures display the Pareto points obtained from both the NMGSO algorithm and the PA-SSP algorithm. It should be mentioned that in each case, the NMGSO algorithm is tested ten times, and the best results are selected. If the number of sensors is notably small, the exact Pareto front can be also calculated with an exhaustive search (ES). In Figs. 4(a) and 4(b), the exact Pareto front is also shown. It can be observed from Figs. 4(a) and 4(b) that the Pareto front provides a wide variety of Pareto optimal sensor configurations. Because it is different from the traditional OSP problem in which there is only one optimal sensor configuration, a set of Pareto solutions exist in the information-entropy-based OSP problem. In this work, only a subset of Pareto points is plotted in the figure such that the data points can be displayed clearly. When the number of sensors that must

be placed is small, e.g., one sensor and three sensors, both the NMGSO algorithm and the PA-SSP algorithm can find the exact Pareto solutions, as shown in Figs. 4(a) and 4(b). And when the number of sensors that must be placed is large, the information entropy indices of the optimal sensor configurations calculated by the PA-SSP algorithm are higher than that extracted by the NMGSO algorithm, as shown in Fig. 4(c)-(f). Therefore, the optimal sensor configurations extracted by the NMGSO algorithm are closer to the exact Pareto front because the PA-SSP algorithm eliminates many meaningful solutions such that feasible solutions in the search space are limited and the iterations can continue. The larger the number of sensors, the greater the number of meaningful solutions eliminated, and thus, the degree of deviation increases with the increasing sensor number. The NMGSO algorithm, which searches the optimal sensor configurations randomly and blindly, is immune to the sensor number and structural properties. Even with a large number of sensors, this algorithm can converge to the Pareto front with high accuracy. Thus, the proposed NMGSO algorithm provides an effective method for finding the optimal sensor configurations for the information-entropy-based OSP problem. The optimal sensor locations of the Pareto points marked in Fig. 4 for 5, 10, and 20 sensors are listed in Table 1.

In the PA-SSP algorithm, the sensors are placed one by one. The feasible solutions increase dramatically with the increase in the number of sensors, which accordingly increase the time required to search the Pareto solutions. Pruning the Pareto set can improve the computational speed. However, certain useful Pareto solutions are lost, and the precision is reduced. Even so, the calculation is time-consuming, especially for large-scale structures with a large number of measured and measurable DOFs. It is well known that a dense distribution of sensors for structural condition assessment is an inevitable trend in the field of SHM (Spencer *et al*. 2004).

The iteration numbers of the NMGSO algorithm for 1, 3, 5, 10, 20, and 30 sensors are approximately 1, 10, 30, 100, 500, and 1000, respectively. Although the iteration number grows with the increasing number of sensors, multi-point, parallel, global, and random search mechanisms enable 1000 iterations to finish in tens of seconds, which demonstrates a high computational efficiency.

Table 1 Optimal sensor locations for 5, 10, and 20 sensors and for the Pareto points marked in Fig. 4

Sensor number	Method	Optimal sensor locations																			
5 sensors	NMGSO	24	37	47	43	70															
	PA-SSP	24	37	47	43	70															
10 sensors	NMGSO	25	26	33	46	48	49	62	66	68	69										
	PA-SSP	25	26	29	35	43	46	50	51	69	70										
20 sensors	NMGSO	10	16	25	26	33	35	37	43	45	48	49	50	52	54	56	61	62	63	70	80
	PA-SSP	24	25	26	27	29	30	33	45	46	47	50	55	62	65	66	68	69	70	73	80

*The numbers in the table denote the serial number of the DOFs counted from the left tower

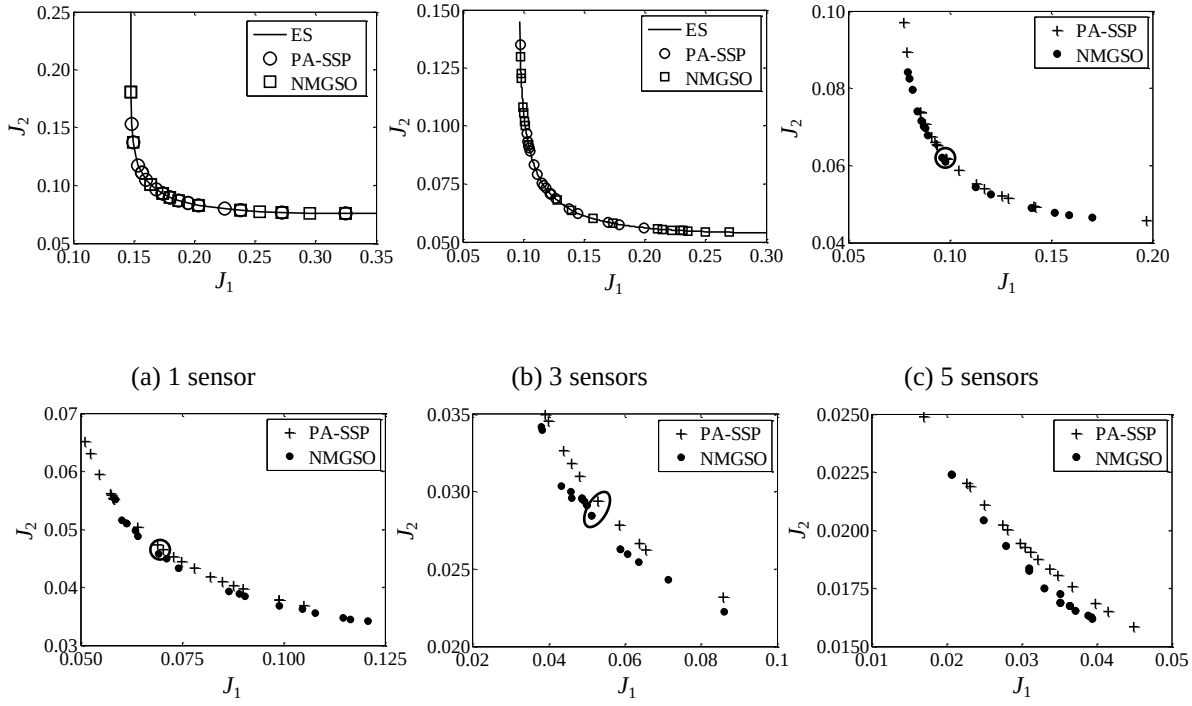

(a) 1 sensor (b) 3 sensors (c) 5 sensors

(d) 10 sensors (e) 20 sensors (f) 30 sensors

Fig. 4 Pareto front for optimal sensor configurations

5. Conclusions

Identifying the parameters of large-scale structures with fewer uncertainties is significant for structural condition assessment in SHM. The information entropy, which is a unique scalar measure of the uncertainties in the estimate of the structural parameters, provides a rational objective for the OSP problem. When information entropy is introduced, the OSP problem becomes a multi-objective optimization problem with discrete variables. In this paper, an NMGSO algorithm based on the basic GSO algorithm is proposed for extracting the Pareto sensor configurations. Selected improvements, i.e., the coding system, the distance, the luciferin definition, and nondirective movement, are developed such that the concept of the basic GSO algorithm can be applied to the information-entropy-based OSP problem. From the numerical simulation, certain conclusions and recommendations are summarized as follows.

(1) The locations of the glowworms in the basic GSO algorithm are coded by real vectors, which cannot be directly implemented in the OSP problem with discrete variables. To overcome this hurdle, the one-dimensional binary coding system is adopted in the NMGSO algorithm. Each glowworm represents a feasible sensor configuration. The location of the glowworm is coded by a binary permutation. Accordingly, the Euclidean distance is replaced by the Hamming distance,

which exactly describes the difference between two feasible sensor configurations.

(2) Non-dominated sorting is introduced to distinguish the glowworms. Two indices, i.e., the RV and the CD, are used to evaluate the superiority or inferiority of a glowworm. Subsequently, the luciferin level of a glowworm is defined as a function of the RV and the CD. Thus, the neighbors of a glowworm can be found conveniently, and comparison of conflicting objective functions is effectively avoided. The movement scheme of a glowworm is converted to relocate certain incongruous sensors for which the number of incongruous sensors is selected randomly. This nondirective movement is particularly effective in maintaining the diversity of glowworms in the population.

(3) Finding the Pareto solutions of the information-entropy-based OSP problem is a challenging task if the number of measurable DOFs and the number of sensors that must be placed are large. The derivative-free and meta-heuristic searching mechanism makes the NMGSO algorithm immune to the sensor number and structural properties. The numerical simulation results indicate that the NMGSO algorithm can effectively converge to the solutions that infinitesimally approach the exact Pareto front. The NMGSO algorithm outperforms the PA-SSP algorithm both in computational accuracy and efficiency, as demonstrated in the numerical example.

It should be noted that the GSO algorithm is a high-performance optimization method, and this paper represents only an elementary attempt to apply this concept to the OSP problem. Further developments will be carried out in future research.

Acknowledgments

This research work was jointly supported by the National Natural Science Foundation of China (Grant No., 51308186, 51421064, 51222806, 51478081), the Natural Science Foundation of Jiangsu Province of China (Grant no. BK20130850), and the Research Fund of State Key Laboratory for Disaster Reduction in Civil Engineering (Grant No. SLDRCE12-MB-03).

References

Arangio, S. and Beck, J.L. (2012), "Bayesian neural networks for bridge integrity assessment", *Struct. Control. Health.*, **19**(1), 3-21.

Azarbayejani, M., El-Osery, A.I., Choi, K.K. and Taha, M.R. (2008), "A probabilistic approach for optimal sensor allocation in structural health monitoring", *Smart. Mater. Struct.*, **17**(5), 055019.

Beck, J.L. and Katafygiotis, L.S. (1998), "Updating models and their uncertainties I: Bayesian statistical framework", *J. Eng. Mech. - ASCE*, **124**(4), 455-461.

Bharat, T.V. (2008), "Agents based algorithms for design parameter estimation in contaminant transport inverse problems", *IEEE Swarm Intelligence Symposium*, USA, 1-7.

Carne, T.G. and Dohmann, C.R. (1995), "A modal test design strategy for modal correlation", *Proceedings of the 13th International Modal Analysis Conference*, USA, 927-933.

Chow, H.M., Lam, H.F., Yin, T. and Au, S.K. (2011), "Optimal sensor configuration of a typical transmission tower for the purpose of structural model updating", *Struct. Control. Health.*, **18**(3), 305-320.

Deb, K., Pratap, A., Agarwal, S. and Meyarivan, T.A.M.T. (2002), "A fast and elitist multiobjective genetic algorithm: NSGA-II", *IEEE. T. Evolut. Comput.*, **6**(2), 182-197.

Flynn, E.B. and Todd, M.D. (2010), "A Bayesian approach to optimal sensor placement for structural health monitoring with application to active sensing", *Mech. Syst. Signal. Pr.*, **24**(4), 891-903.

Fonseca, C.M. and Fleming, P.J. (1995), "An overview of evolutionary algorithms in multiobjective optimization", *Evolutionary Comput.*, **3**(1), 1-16.
Friswell, M. and Mottershead, J. E. (1995), *Finite Element Model Updating in Structural Dynamics*, Kluwer Academic Publishers.
Gong, Q., Zhou, Y. and Luo, Q. (2011), "Hybrid artificial glowworm swarm optimization algorithm for solving multi-dimensional knapsack problem", *Procedia Engineering*, **15**, 2880-2884.
Hamming, R.W. (1950), "Error detecting and error correcting codes", *Bell. System. Technical. J.*, **29**(2), 147-160.
Heredia-Zavoni, E. and Esteva, E.L. (1998), "Optimal instrumentation of uncertain structural systems subject to earthquake ground motions", *Earthq. Eng. Struct. D.*, **27**(4), 343-362.
Huang, K., Zhou, Y. and Wang, Y. (2011), "Niching glowworm swarm optimization algorithm with mating behavior", *J. Inform.Comput. Sci,*, **8**, 4175-4184.
Jaynes, E.T. (1978), "Where do we stand on maximum entropy", *The maximum entropy formalism*, **15**, 118.
Kammer, D.C. (1991), "Sensor placement for on-orbit modal identification and correlation of large space structures", *J. Guid. Control. Dynam.*, **14**(2), 251-259.
Kang, F., Li, J.J. and Xu, Q. (2008), "Virus coevolution partheno-genetic algorithms for optimal sensor placement", *Adv. Eng. Inform.*, **22**(3), 362-370.
Kang, F., Li, J. and Li, H. (2013), "Artificial bee colony algorithm and pattern search hybridized for global optimization", *Appl. Soft. Comput.*, **13**(4), 1781-1791.
Konak, A., Coit, D.W. and Smith, A.E. (2006), "Multi-objective optimization using genetic algorithms: A tutorial", *Reliab. Eng. Syst. Safe*, **91**(9), 992-1007.
Krishnanand, K.N. and Ghose, D. (2005), "Detection of multiple source locations using a glowworm metaphor with applications to collective robotics", *IEEE swarm intelligence symposium*, California, USA, 84-91.
Krishnanand, K.N. and Ghose, D. (2009), "Glowworm swarm optimization for simultaneous capture of multiple local optima of multimodal functions", *Swarm Intelligence*, **3**(2), 87-124.
Liao, W.H., Kao, Y. and Li, Y.S. (2011), "A sensor deployment approach using glowworm swarm optimization algorithm in wireless sensor networks", *Expert Systems with Applications*, **38**(10), 12180-12188.
Li, J. and Law, S.S. (2012a), "Damage identification of a target substructure with moving load excitation", *Mech. Syst. Signal. Pr.*, **30**, 78-90.
Li, J., Law, S.S. and Ding, Y. (2012b), "Substructure damage identification based on response reconstruction in frequency domain and model updating", *Eng. Struct.*, **41**, 270-284.
Mufti, A.A. (2002), "Structural health monitoring of innovative Canadian civil engineering structures", *Struct. Health. Monit.*, **1**(1), 89-103.
Ngatchou, P.N., Fox, W.L. and El–Sharkawi, M.A. (2005), "Distributed sensor placement with sequential particle swarm optimization", *Swarm Intelligence Symposium, Proceedings 2005 IEEE*, 385-388.
Nie, H., Shen, J. and Li, X. (2014), "Research on glowworm swarm optimization with ethnic division", *J. Networks*, **9**(2), 458-465.
Ntotsios, E., Christodoulou, K. and Papadimitriou, C. (2006), "Optimal sensor location methodology for structural identification and damage detection", *Proceedings of the 3rd European Workshop on Structural Health Monitoring*, Granada, Spain.
Papadimitriou, C., Beck, J.L. and Au, S.K. (2000), "Entropy-based optimal sensor location for structural model updating", *J. Vib. Control.*, **6**(5), 781-800.
Papadimitriou, C. (2004), "Optimal sensor placement methodology for parametric identification of structural systems", *J. Sound. Vib.*, **278**(4), 923-947.
Papadimitriou, C. (2005), "Pareto optimal sensor locations for structural identification", *Comput. Method. Appl. M.*, **194**(12-16), 1655-1673.
Shi, Z.Y., Law, S.S. and Zhang, L.M. (2000), "Optimum sensor placement for structural damage detection", *J. Eng. Mech. - ASCE*, **126**(11), 1173-1179.
Spencer, B.F., Ruiz-Sandoval, M.E. and Kurata, N. (2004), "Smart sensing technology: opportunities and

challenges", *Struct. Control. Hlth.*, **11**(4), 349-368.
Udwadia, F.E. (1994), "Methodology for optimal sensor locations for parameter identification in dynamic systems", *J. Eng. Mech.- ASCE*, **120**(3), 68-90.
Yang, Y., Zhou, Y. and Gong, Q. (2010), "Hybrid artificial glowworm swarm optimization algorithm for solving system of nonlinear equations", *J. Comput. Inform. Syst.*, **6**(10), 3431-3438.
Yao, L., Sethares, W.A. and Kammer, D C. (1993), "Sensor placement for on orbit modal identification via a genetic algorithm". *AIAA J*., **31**(10), 1922-1928.
Ye, S.Q. and Ni, Y.Q. (2012), "Information entropy based algorithm of sensor placement optimization for structural damage detection", *Smart. Struct. Syst.*, **10**(4-5), 443-458.
Yi, T.H., and Li, H.N. (2012), "Methodology developments in sensor placement for health monitoring of civil infrastructures", *Int. J. Distrib. Sens. N.*, Article ID 612726
Yi, T.H., Li, H.N. and Gu, M. (2011a), "Optimal sensor placement for health monitoring of high-rise structure based on genetic algorithm", *Math. Probl. Eng.*, Article ID 395101.
Yi, T.H., Li, H.N. and Gu, M. (2011b), "Optimal sensor placement for structural health monitoring based on multiple optimization strategies. *Struct. Des. Tall. Spec.*, **20**(7), 881-900.
Yi, T. H., Li, H. N. and Gu, M. (2013), "Recent research and applications of GPS-based monitoring technology for high-rise structures", *Struct. Control. Health.*, **20**(5), 649-670.
Yi, T.H., Li, H.N. and Zhang, X.D. (2012a). "A modified monkey algorithm for optimal sensor placement in structural health monitoring", *Smart. Mater. Struct.*, **21**(10), 105033.
Yi, T.H., Li, H.N. and Zhang, X.D. (2012b), "Sensor placement on Canton Tower for health monitoring using asynchronous-climb monkey algorithm", *Smart. Mater. Struct.*, **21**(12), 125023.
Yuen, K.V., Katafygiotis, L.S., Papadimitriou, C. and Mickleborough, N.C. (2001), "Optimal sensor placement methodology for identification with unmeasured excitation," *J. Dyn. Syst-T. Asme.*, **123**(4), 677-686.
Zainal, N., Zain, A.M., Radzi, N.H.M. and Udin, A. (2013), "Glowworm swarm optimization (GSO) algorithm for optimization problems: A state-of-the-art review", *Appl. Mech. Mater.*, 421, 507-511.
Zhou, G.D. and Yi, T.H. (2013a), "Recent developments on wireless sensor networks technology for bridge health monitoring", *Math. Probl. Eng.*, Article ID 947867.
Zhou, G.D. and Yi, T.H. (2013b), "Thermal load in large-scale bridges: a state-of-the-art review", *Int. J. Distrib. Sens. N.*, Article ID 797650.
Zhou, G.D. and Yi, T.H. (2013c), "The nonuniform node configuration of wireless sensor networks for long-span bridge health monitoring", *Int. J. Distrib. Sens. N.*, Article ID 797650.
Zhou, G.D. and Yi, T.H. (2013d), "The node arrangement methodology of wireless sensor networks for long-span bridge health monitoring", *Int. J. Distrib. Sens. N.*, Article ID 865324.
Zhou, Y., Zhou, G., Wang, Y. and Zhao, G. (2013), "A glowworm swarm optimization algorithm based tribes", *Appl. Math. Inform. Sci.*, **7**(2), 537-541.